

Mechanochemical Approach to Gallate BioMOFs: Efficient Synthesis and Cr(VI) Removal from Aqueous and Soil Systems

*Alisson Luiz Rocha Balbino^{†a}, Giovanna Pereira Correia^{†a}, Gustavo Henrique Correia dos Santos^a, Priscilla Jussiane Zambiasi^a, João Paulo da Silva Souza^a, Bryan Alberto Laura Larico^a, Denise de Lima Dias Delarica^b, Kathleen Fernandes^b, Mara Regina Moitinho^b, Luciana Pires Rodrigues Betioli^b, José Marques Junior^b, Dagoberto de Oliveira da Silva^c, Paulo Filho Marques de Oliveira^a and Liane Marcia Rossi^{*a}*

^aDepartamento de Química Fundamental, Instituto de Química, Universidade de São Paulo, Av. Prof. Lineu Prestes 748 sl. 1265, 05508-000, São Paulo, Brazil

^bSchool of Agricultural and Veterinary Sciences, São Paulo State University (FCAV-UNESP), Via de Acesso Prof. Paulo Donato Castellane, s/n, Jaboticabal, São Paulo, Brazil.

^cMOF TECH Pesquisa & Desenvolvimento Ltda., Rua Cônego José Marinho, 77/112, 05337-080, São Paulo, Brazil

[†]These authors contributed equally to this work.

Calculation of reaction yields

Fe-Gallate MOF

Assumptions. Product formula: $\text{Fe}(\text{C}_7\text{O}_5\text{H}_3)$ (1 Fe: 1 ligand : 1 product). Reagents: gallic acid monohydrate ($\text{C}_7\text{H}_6\text{O}_5 \cdot \text{H}_2\text{O}$), $\text{FeCl}_2 \cdot 4\text{H}_2\text{O}$, NaOH. Masses reagents used: 0.720 g gallic acid monohydrate, 0.400 g $\text{FeCl}_2 \cdot 4\text{H}_2\text{O}$, 0.240 g NaOH. Isolated product masses after washing and drying (corresponding to different milling times) are given below.

Molar masses (used):

$$\text{C}_7\text{H}_6\text{O}_5 \cdot \text{H}_2\text{O} = 188.135 \text{ g} \cdot \text{mol}^{-1}; \text{FeCl}_2 \cdot 4\text{H}_2\text{O} = 198.811 \text{ g} \cdot \text{mol}^{-1}; \text{Fe}(\text{C}_7\text{O}_5\text{H}_3) = 222.941 \text{ g} \cdot \text{mol}^{-1}.$$

Moles of reagents added:

$$n(\text{gallic acid monohydrate}) = 0.720 \text{ g} \div 188.135 \text{ g} \cdot \text{mol}^{-1} = 0.0038270 \text{ mol}$$

$$n(\text{FeCl}_2 \cdot 4\text{H}_2\text{O}) = 0.400 \text{ g} \div 198.811 \text{ g} \cdot \text{mol}^{-1} = 0.0020120 \text{ mol (limiting reagent)}$$

$$n(\text{NaOH}) = 0.240 \text{ g} \div 39.997 \text{ g} \cdot \text{mol}^{-1} = 0.0060005 \text{ mol}$$

Theoretical mass of product (maximum)

$$\text{Moles of product (max)} = \text{moles of limiting reagent} = 0.0020120 \text{ mol}$$

$$\text{Theoretical mass} = 0.0020120 \text{ mol} \times 222.941 \text{ g} \cdot \text{mol}^{-1} = 0.44856 \text{ g}$$

Table SI 1. Isolated masses and yields (by milling time) for Fe-Gallate MOF

Milling time (min)	Isolated mass (g)	Yield (%) = (mass / 0.44856) × 100
90	0.414	92.3 %
60	0.411	91.6 %
30	0.310	69.1 %
15	0.285	63.5 %

Mg-Gallate MOF

Assumptions. Product formula: $\text{Mg}(\text{C}_7\text{O}_5\text{H}_4)$ (1 Mg : 1 ligand : 1 product). Reagents: gallic acid monohydrate ($\text{C}_7\text{H}_6\text{O}_5 \cdot \text{H}_2\text{O}$), $\text{MgSO}_4 \cdot 7\text{H}_2\text{O}$, NaOH. Masses of reagents used: 0.670 g gallic acid monohydrate, 0.460 g $\text{MgSO}_4 \cdot 7\text{H}_2\text{O}$, 0.223 g NaOH. Isolated product masses after washing and drying (corresponding to different milling times) are given below.

Molar masses (used):

- $\text{C}_7\text{H}_6\text{O}_5 \cdot \text{H}_2\text{O} = 188.135 \text{ g} \cdot \text{mol}^{-1}$
- $\text{MgSO}_4 \cdot 7\text{H}_2\text{O} = 246.471 \text{ g} \cdot \text{mol}^{-1}$
- $\text{Mg}(\text{C}_7\text{O}_5\text{H}_4) = 192.409 \text{ g} \cdot \text{mol}^{-1}$

Moles of reagents added:

- $n(\text{gallic acid monohydrate}) = 0.670 \text{ g} \div 188.135 \text{ g} \cdot \text{mol}^{-1} = 0.0035613 \text{ mol}$
- $n(\text{MgSO}_4 \cdot 7\text{H}_2\text{O}) = 0.460 \text{ g} \div 246.471 \text{ g} \cdot \text{mol}^{-1} = 0.0018663 \text{ mol}$ (limiting reagent)
- $n(\text{NaOH}) = 0.223 \text{ g} \div 39.997 \text{ g} \cdot \text{mol}^{-1} = 0.0055754 \text{ mol}$

Theoretical mass of product (maximum)

Moles of product (max) = moles of limiting reagent = 0.0018663 mol

Theoretical mass = $0.0018663 \text{ mol} \times 192.409 \text{ g} \cdot \text{mol}^{-1} = 0.35910 \text{ g}$

Table SI 2. Isolated masses and yields (by milling time) for Mg-Gallate MOF

Milling time (min)	Isolated mass (g)	Yield (%) = $(\text{mass} / 0.44856) \times 100$
90	0.270	75.2 %
60	0.243	67.7 %
30	0.200	55.7 %
15	0.039	10.9 %

Refinements

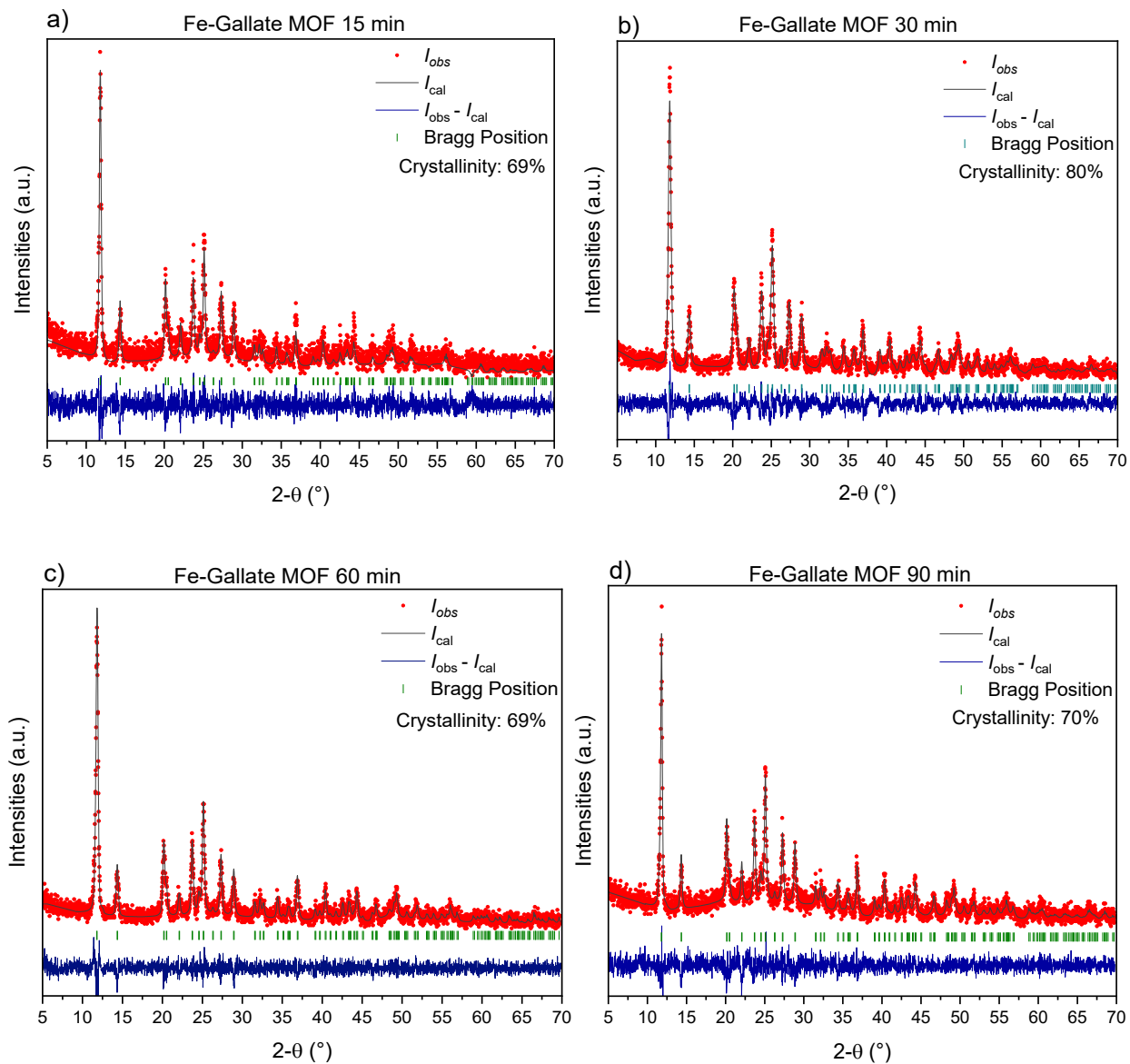


Fig. S1 Refinement for Fe-Gallate MOF at synthesis times of 15 (a) 30 (b), 60 (c), and 90 min (d).

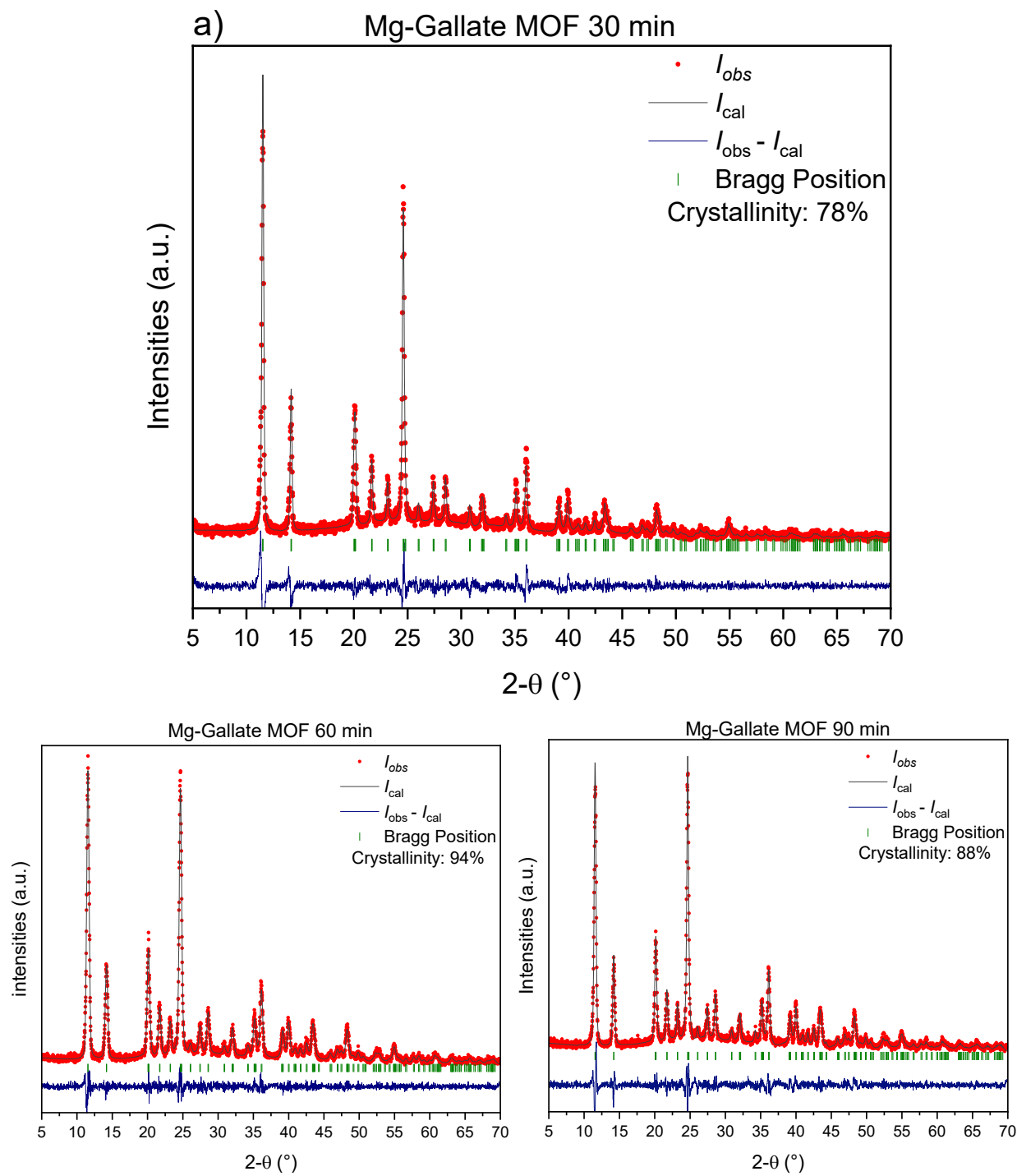


Fig. S2 Refinement for Mg-Gallate MOF at synthesis times of 30 (a), 60 (b), and 90 min (c).

Table SI 3. Unit cell and refinement parameters obtained from the Rietveld method for Fe-Gallate and Mg-Gallate materials were obtained for each mechanochemical reaction time. Rietveld refinement was performed based on crystallographic data obtained from model reference structures (CCDC Code 1260549 and 1899504).

Fe-Gallate MOF					Mg-Gallate MOF		
	15 min	30 min	60 min	90 min	30 min	60 min	90 min
Cell Parameters – Space Group <i>P3₁21</i> (152)							
<i>a</i> (Å)	8.659(6)	8.651(5)	8.658(6)	8.673(5)	8.868(3)	8.849(3)	8.848(3)
<i>b</i> (Å)	8.659(6)	8.651(5)	8.658(6)	8.673(5)	8.868(3)	8.849(3)	8.848(3)
<i>c</i> (Å)	10.877(17)	10.88(11)	10.86(12)	10.88(11)	10.772(8)	10.765(9)	10.764(8)
$\alpha = \beta = 0^\circ$							
$\gamma = 120^\circ$							
Rietveld R- factors for Pattern	$R_p = 17.15$	$R_p = 18.1$	$R_p = 18.1$	$R_p = 16.1$	$R_p = 12.7$	$R_p = 12.86$	$R_p = 13.75$
	$R_{wp} = 21.85$	$R_{wp} = 23.1$	$R_{wp} = 23.1$	$R_{wp} = 20.5$	$R_{wp} = 16.9$	$R_{wp} = 16.4$	$R_{wp} = 17.26$
χ^2	1.68	1.96	1.73	1.60	2.29	2.73	2.63

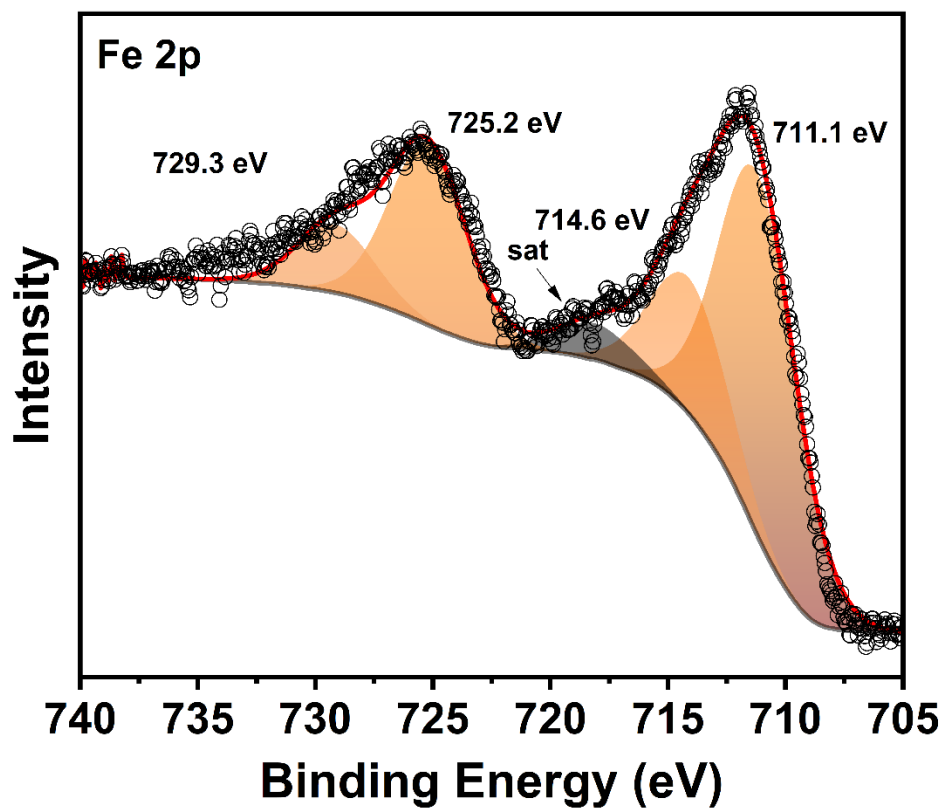


Fig. S3 High Resolution XPS spectrum of Fe-Gallate MOF in the Fe 2p region.

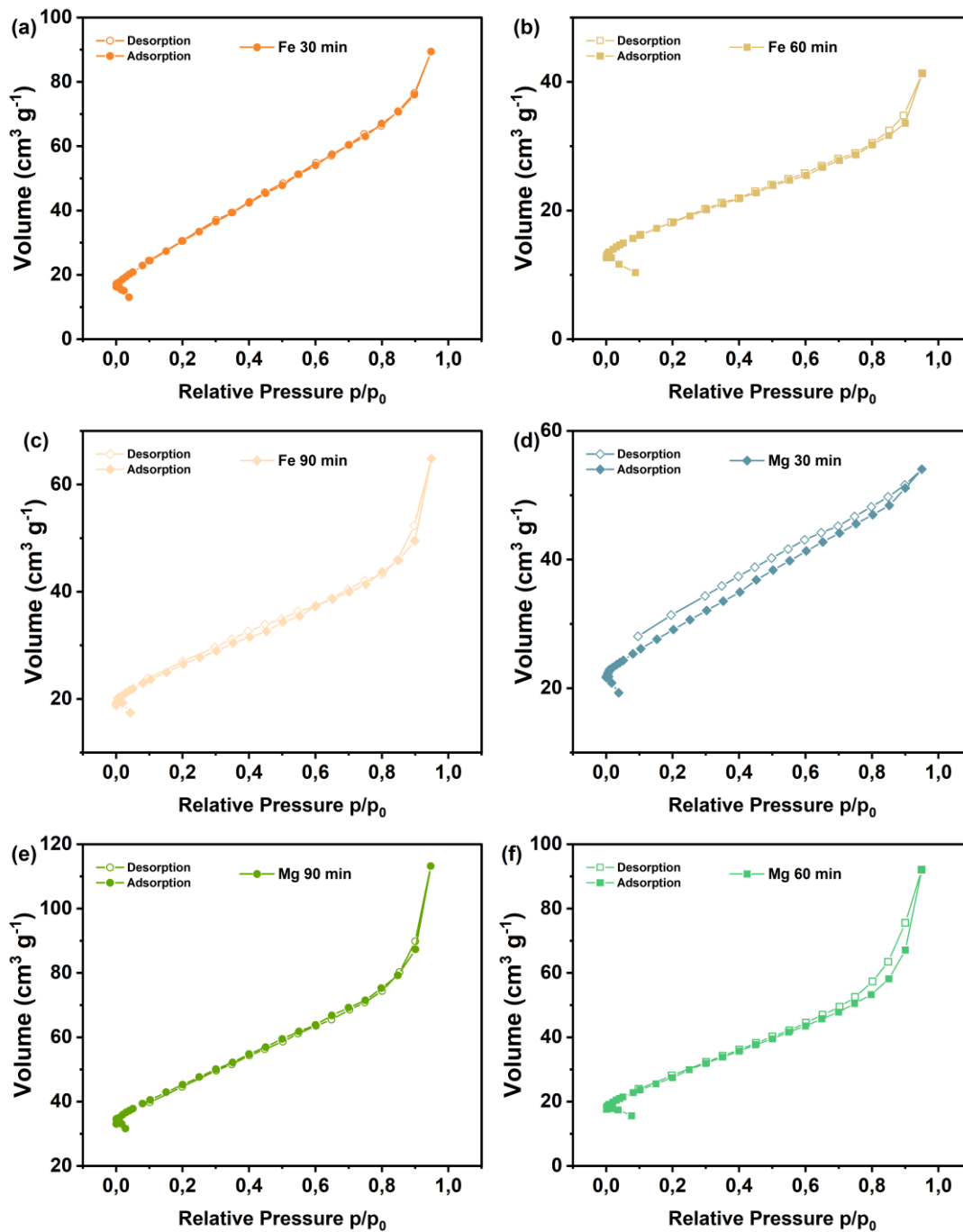


Fig. S4 N_2 adsorption-desorption isotherms of (a – c) Fe-Gallate MOF, and (d – f) Mg-Gallate MOF at synthesis times of 30, 60, and 90 min.

Analysis of residues obtained after thermal decomposition

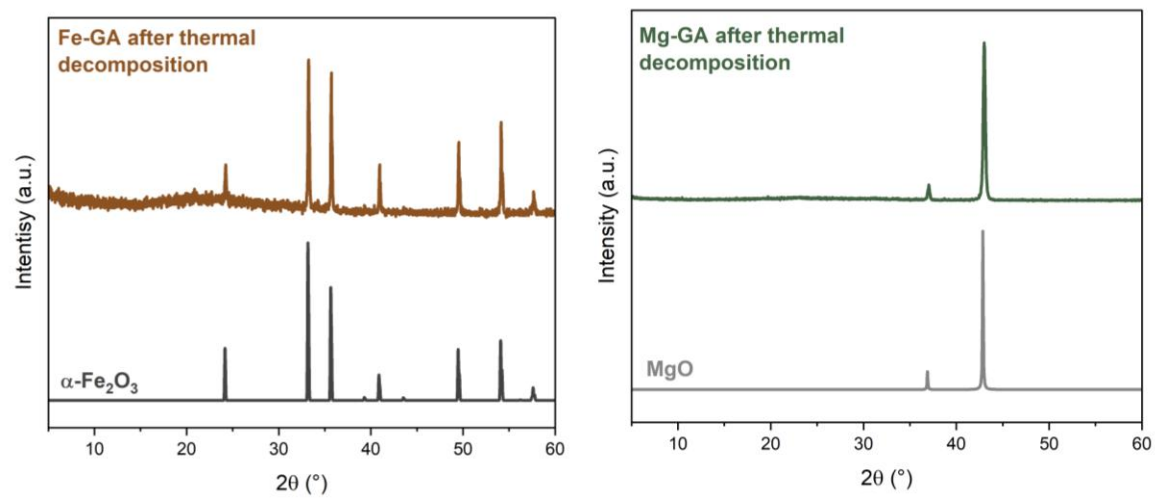


Fig. S5 XRD pattern obtained after thermal decomposition of Fe-GA (a) and Mg-GA (b)

Kinetic Adsorption

To compare the adsorption process of Fe-Gallate and Mg-Gallate MOF, four adsorption kinetics models were analysed: pseudo-first-order, pseudo-second-order, intraparticle diffusion and Elovich kinetic models, shown respectively in equations 1-4.¹⁻³ All the plots are shown in Figure S6, while the correlation coefficients as well the kinetics constants and Q_e values are shown **Table SI 4**.

Pseudo-First Order (Lagergren Model)

The pseudo-first-order kinetics is applicable if the plot $\ln(q_e - q_t)$ against time (t) shows a linear relationship, in which the slope indicates the k_1 , and the interception the $\ln(q_e)$. The model suggests a phenomenon of adsorption based on physical interaction.

$$\ln(q_e - q_t) = \ln q_e - k_1 t \quad (1)$$

q_e = quantity absorbed in the equilibrium (mg/g)

q_t = quantity absorbed in a giving time t

k_1 = velocity constant of a pseudo-first order system

Pseudo-Second Order (Ho and Mckay Model)

The pseudo-second order kinetics is applicable if the plot $\frac{t}{q_t}$ against time (t) shows a linear relationship, in which the slope indicates the $\frac{1}{q_e}$, and the interception $\frac{1}{k_2 q_e^2}$. The model suggests a phenomenon of adsorption based on chemical interaction.

$$\frac{t}{q_t} = \frac{1}{k_2 q_e^2} + \frac{t}{q_e} \quad (2)$$

k_2 = velocity constant of a pseudo-second order system

Elovich Model

The Elovich kinetics is applicable if the plot q_t against $\ln(t)$ show a linear relationship, in which the slope indicates $\frac{1}{\beta}$ and the interception $\frac{1}{\beta} \ln(\alpha\beta)$. The model suggests a phenomenon of adsorption based on chemical adsorption, strongly influenced by the morphology of the material, with heterogeneous active sites, which can occur both on the surface and within the pores.

$$q_t = \frac{1}{\beta} \ln(\alpha\beta) + \frac{1}{\beta} \ln(t) \quad (3)$$

q_t = quantity absorbed in a giving time t

α = initial adsorption ratio (mg/g.min)

β = related to the activation energy and complexity of the surface

Intraparticle diffusion (Weber-Morris)

The Weber-Morris kinetics is applicable if the plot q_t against $t^{1/2}$ show a linear relationship, in which the slope indicates k_{id} and the interception C . The model suggests a phenomenon of adsorption in multiple steps, in which the intraparticle diffusion may be the limiting factor.

$$q_t = k_{id}t^{1/2} + C \quad (4)$$

q_t = quantity absorbed in a giving time t

k_{id} = constant of the intraparticle diffusion ratio (mg/g.min^{1/2})

C = constant related with the limitant layer width

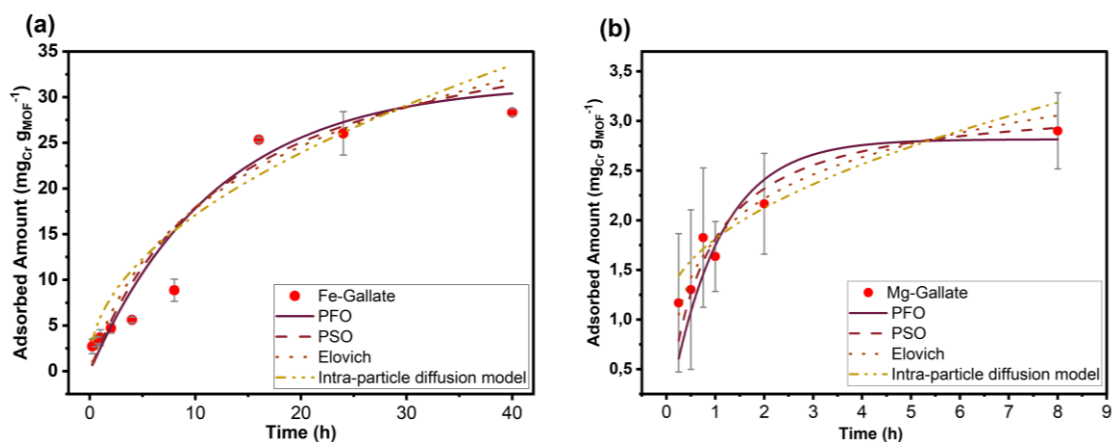


Fig. S6 Fitting of Cr adsorption kinetics by Fe-Gallate (a) and Mg-Gallate MOF (b). Pseudo-first (PFO) and Pseudo-second order (PSO); Intra-particle diffusion or Weber-Moris model and Elovich model.

Table SI 4: Values obtained for Fe-Gallate and Mg-Gallate MOF by pseudo-first, pseudo-second-order, Weber-Moris and Elovich kinetics for Chromium adsorption

Fe-Gallate MOF			Mg-Gallate MOF		
Pseudo-First Order			Pseudo-First Order		
Q _e = 31.52	K ₁ = 0.0834	R ² = 0.9441	Q _e = 2.8150	K ₁ = 0.9682	R ² = 0.8446
Pseudo-Second Order			Pseudo-Second Order		
Q _e = 41.67	K ₂ = 0.0018	R ² = 0.9970	Q _e = 3.2130	K ₂ = 0.4028	R ² = 0.9705
Elovich			Elovich		
α ≈ 4.1270	β = 0.0844	R ² = 0.9972	α ≈ 11.1270	β = 1.6320	R ² = 0.9751
Weber-Moris			Weber-Moris		
K _{id} = 5.1930	C = 0.6832	R ² = 0.9871	K _{id} = 0.7510	C = 1,0617	R ² = 0.9690

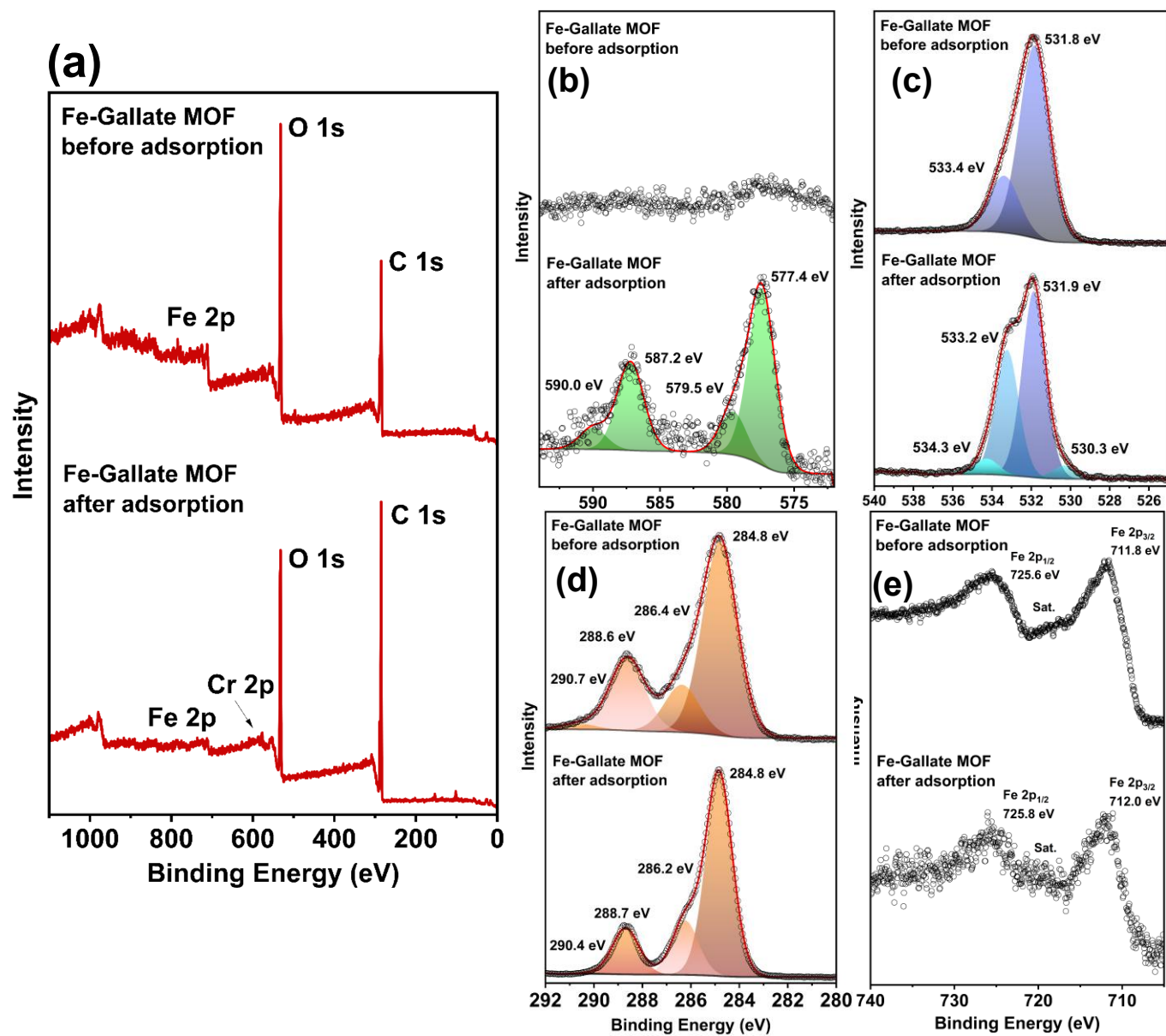


Fig S7 XPS spectra of Fe-Gallate MOF before and after the Cr adsorption

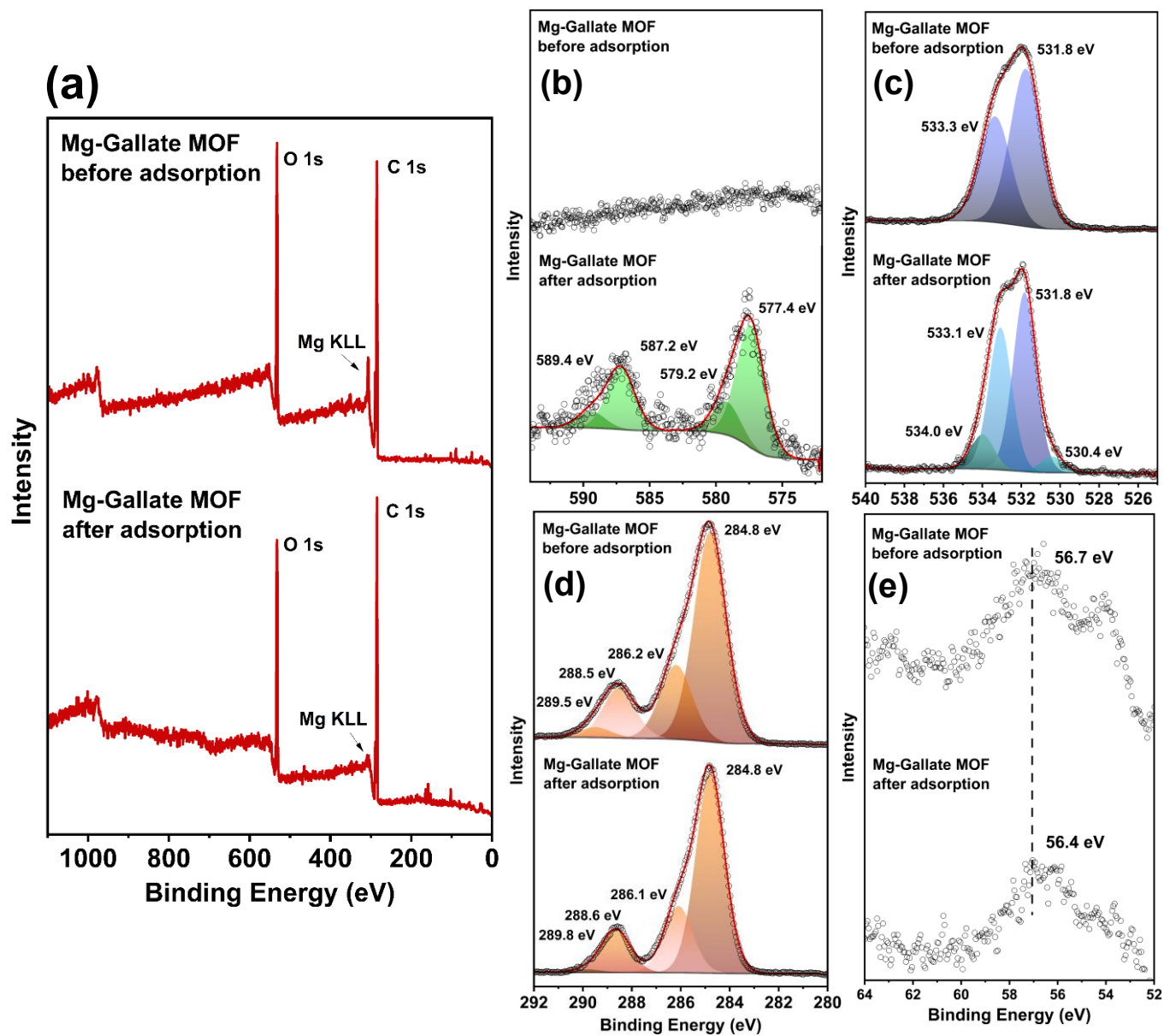


Fig S8 XPS spectra of Mg-Gallate MOF before and after the Cr adsorption

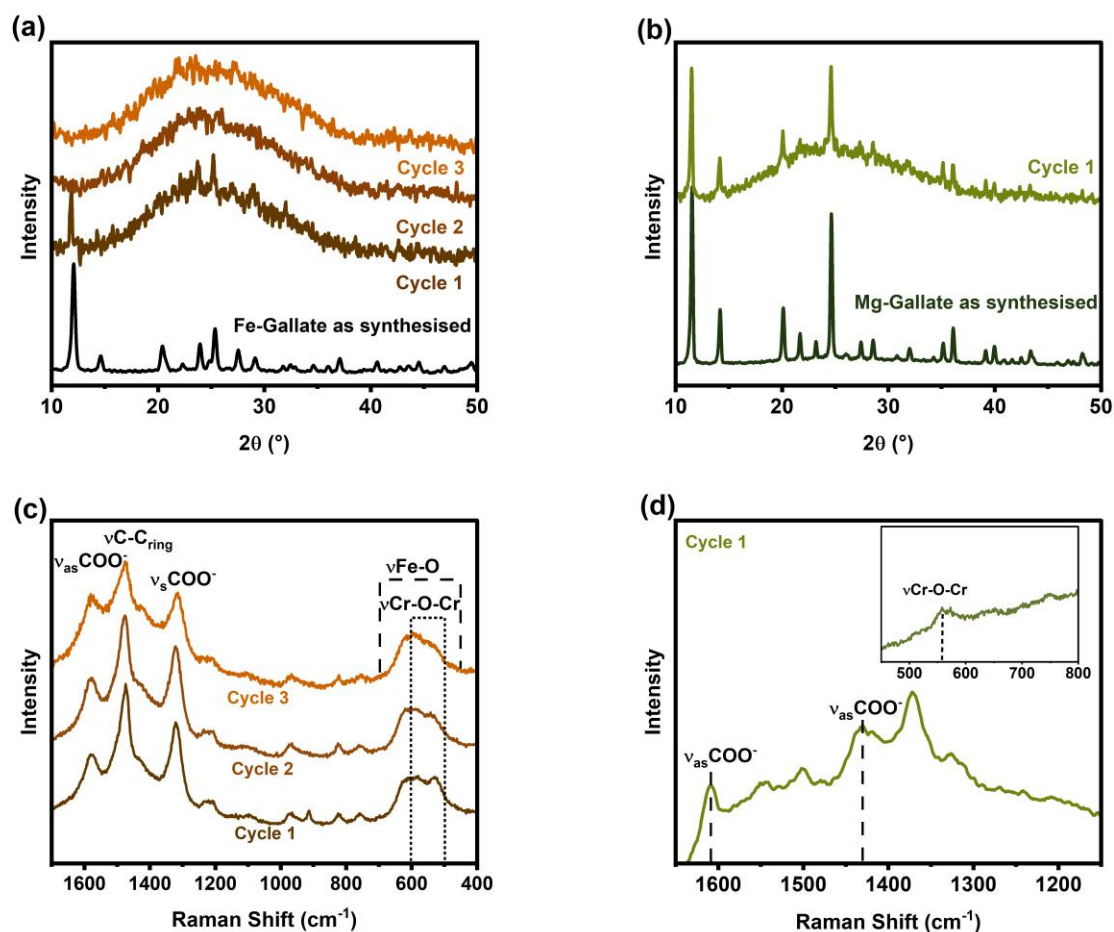


Fig. S9 Characterization of samples after three cycles of Cr adsorption (a) PXRD pattern and (c) Raman spectra of Fe-Gallate from 1700 to 400 cm^{-1} (b) PXRD pattern and (d) Raman spectra of Mg-Gallate from 1700 to 400 cm^{-1} .

References

- 1 H. Wang, W. Wang, S. Zhou and X. Gao, *Heliyon*, 2023, **9**, e13267.
- 2 M. N. Uddin, G. C. Saha, M. A. Hasanath, M. A. H. Badsha, M. H. Chowdhury and A. R. Md. T. Islam, *PLoS One*, 2023, **18**, e0290234.

- 3 H. P. Nogueira, S. H. Toma, A. T. Silveira, A. A. C. Carvalho, A. M. Fioroto and K. Araki,
Microchemical Journal, 2019, **149**, 104025.